BULLETIN OF THE POLISH ACADEMY OF SCIENCES
TECHNICAL SCIENCES, Vol. 68, No. 6, 2020
DOI: 10.24425/bpasts.2020.135390

ELECTRONICS, TELECOMMUNICATION
AND OPTOELECTRONICS

Analog circuits specification driven testing by means of digital stream and non-linear estimation model optimized evolutionarily

T. GOLONEK* and Ł. CHRUSZCZYK

Faculty of Automatic Control, Electronics and Computer Science, Silesian University of Technology,
ul. Akademicka 16, 44-100 Gliwice, Poland

Abstract. The method described in this work allows to determine the optimal distribution of pulses of digital signal as well as the non-linear mathematical model based on a multiple regression statistical analysis, which are specialized to an effective and low-cost testing of functional parameters in analog electronic circuits. The aim of this concept is to simplify the process of analog circuit specification validation and minimize hardware implementation, time and memory requirements during the testing stage. This strategy requires simulations of the analyzed analog electronic circuit; however, this effort is done only once – before the testing stage. Then, validation of circuit specification can be obtained after a quick, very low-cost procedure without time consuming computations and without expensive external measuring equipment usage. The analyzed test signature is a time response of the analog circuit to the stream of digital pulses for which distributions were determined during evolutionary optimization cycles. Besides, evolutionary computations assure determination of the optimal form and size of the non-linear mathematical formula used to estimate specific functional parameters. Generally, the obtained mathematical model has a structure similar to the polynomial one with terms calculated by means of multiple regression procedure. However, a higher ordered polynomial usage makes it possible to reach non-linear estimation model that improves accuracy of circuit parametric identification. It should be noted that all the evolutionary calculations are made only at the *before test stage* and the main computational effort, for the analog circuit specification test design, is necessary only once. Such diagnosing system is fully synchronized by a global digital signal clock that precisely determines time points of the slopes of input excitation pulses as well as acquired output signature samples. Efficiency of the proposed technique is confirmed by results obtained for examples based on analog circuits used in previous (and other) publications as test benchmarks.

Key words: analog electronic circuits, specification driven testing, evolutionary computations, multiple regression.

1. Introduction

Specification testing and fault diagnosis are important unavoidable parts of manufacturing and lifetime of electronic circuits. Reliability assurance – an important factor of electronic component as part of a system – can and must be achieved by precise control of manufacturing and quality control of the final product. Typically, the test designer must solve contradictory issues:

- efficiency of fault diagnosis: how many faults can be successfully distinguished?
- access to circuit internals: limited and expensive (in terms of external connectors for integrated circuit package),
- component cost: can be reduced by the maximization of component tolerances (in limits defined by specification), but degrades diagnosis efficiency,
- circuit total cost: overhead (in terms of silicon area) caused by *Design-for-Testability* (DfT),
- post-production testing cost: related with test time (single or many measurements? how much data, accuracy or signal processing required?) [1].

As the complexity of electronic circuits and systems increases, the test cost is a significant part of the final cost (30–50% [2, 3]). All abovementioned factors can be modelled as an optimization problem of multiple circuit and testing parameters.

Basically, philosophy of *testing* (sometimes called *validation*) can be divided into:

- specification (functional) testing – design specification (functional parameters) is validated, this implies typically *behavioral testing*,
- fault diagnosis – tries to find if a failure occurred in the circuit (or system). The circuit still can be out of its specifications, but there is no other way, e.g., for single-use systems, where functional test would be destructive.

The most important problems in testing and fault diagnosis of integrated analog electronic circuits (AECs) are the tolerance of component values, limited access to internals nodes. The tolerance of component values (circuit parameters), not really considered in models of digital circuit testing, causes spread of measured parameters and the result is fault masking – overlap (*ambiguity sets*). Decreasing tolerances makes diagnosis easier (to some limits), but at the same time increases manufacturing cost. In case of integrated circuits (IC), no access to internal nodes locks important sources of diagnostic information [1, 4]. Additionally, the fault diagnosis of AEC can have three goals:

- fault detection – distinguishes faulty circuits (NO-GO) from healthy ones (without failures, GO),
- fault location – locates faulty element,
- fault identification – determines value of faulty component (or at least shift below or above tolerance margin).

---

*e-mail: tomasz.golonek@polsl.pl

Manuscript submitted 2020-04-27, revised 2020-09-23, initially accepted for publication 2020-10-12, published in December 2020

Usually, the complete diagnosis steps are detection first → then location → finally identification. Such separation has advantages:

- the fault detection is typically the simplest, shortest and often the only required on production line. If fault probability is low, the further steps are rarely performed;
- simplification of individual steps: e.g., fault detection does not have to distinguish among particular faults; fault location does not have to distinguish a healthy circuit from a faulty one; fault identification does not have to distinguish any faults – only "learn" relation between component value and some observable.

Typically, fault detection is performed during the manufacturing process (production line), while fault location and identification during prototyping/centering or post-production (life stage).

Very important division of fault diagnosis methods is based on types of analyzed signals (excitation and response):

- DC – simplest and shortest but limited by reactive elements. Required test equipment is simple and low-cost [5, 6],
- AC – can also consider faults in reactive components and test equipment is still low-cost. Disadvantage may be longer testing time [7–9],
- time domain – including aperiodic excitation and/or transient response. Carries the most information about circuit and is not limited by circuit linearity. May require expensive test equipment and/or processing (thus testing) time [10–12].

Lately, methods utilizing sophisticated information analysis (or complex design-for-testability of circuit) are used to read as much information from circuit as possible: wavelet transform, evolutionary optimization or artificial intelligence [13–19].

The last important division of fault diagnosis is the moment when faults are modelled and circuit measured:

- Simulate–After–Test (SAT) – response of circuit is taken first, then analysis is made ("on-line"). Usually, the analysis time dominates total test time,
- Simulate–Before–Test (SBT) – faults are modelled (simulated) first and stored in fault dictionary before any measurements ("off-line"). Total test time is determined mainly by measurement time – this is an advantage over SAT methods.

Presented method belongs to the class of functional testing: design specification is validated – though indirectly but is faster and uses simpler resources (hardware and software). The excitation is aperiodic, fully digital and optimized by means of genetic algorithm. The response is analyzed with multiple regression in order to maximize diagnostic information. The process of excitation design and optimization of response analysis is performed off-line (SBT), thus testing time is determined mainly by measurement time. The result is high testing performance at low cost (small silicon area and processing overhead).

Evolutionary algorithms (EAs) are heuristic optimization techniques which imitate natural processes of genetic material recombination and mutation among mating individuals selected with desired pressure. They use the fitness function which consists of criteria optimized during evolutionary cycles constructed respectively to the considered task and this function allows to promote suitable solutions found in wide searching space. The problem solution is coded by means of a set of assumed alleles (genetic alphabet that expresses available values of quants) connected to requested structures (e.g., strings, matrixes, diagram trees) which are chromosomes. The series of chromosomes may be used to obtain a genotype representing more complex task considered to optimization. In literature many varieties of evolutionary techniques may be found: a genetic algorithm, genetic programming, evolutionary strategy or differential evolution. They have some specific individual features (e.g., dedicated structures of genotypes) but generally, all these methods are evolutionary ones basing on the mentioned ideas taken from the nature and they are a projection of rivalry between individuals from the population of candidates. This kind of computations allows to solve different difficult problems [12, 13, 16, 17, 20–25] for which a determined solution, an ideal reference mathematical model cannot be defined or is difficult to obtain. The limitations and challenges specified above for the AECs testing tasks cause artificial intelligence algorithms to be well matched to solve them.

Previously published methods dedicated to the specification driven testing of AECs may be found in works [24–27]. Techniques from [25, 26] use the multivariate adaptive regression splines (MARS) tool to design the tested performance parameters estimation functions. Approach [27] proposes to analyze CUT pulse response selected features and verification of their position's correctness into respective acceptability regions. However, in [24] multiple regression and simple step form of excitation are used. In this work a method that bases on EA (modified version of genetic algorithm) is proposed and it allows to make the design of optimal specification test. The novelty of our method is EA usage to fully complex and automatic design of optimal specification test with minimization of final implementation cost supporting. The number of test points (defines size of the set of measured test response samples which have to be processed) and the quantity of coefficients unequivocally defining specification test procedure (impacts directly to memory requirements for the test implementation) are minimized evolutionarily. The test stimulus (i.e., pulses distribution in the testing stream) as well as the tested performance parameters identification models (i.e., regression functions) are tied and optimized together in the same system. In our opinion, it is the strong new feature of the method. Besides, the multiple regression formula has a unique non-linear form with terms values optimized evolutionarily. Additionally, the size of this mathematical model is also concurrently minimized. All the features mentioned make it possible to design a simple specification test that may be easily implemented with very low cost and this procedure assures quick estimation of actual values of CUT verified performance parameters. All time-consuming calculations are made before the real analog specification test and finally only easily generatable digital excitation and simple analysis of the analog CUT response are used to obtain valuable diagnostic information. The simplicity of the specification test procedure predisposes this method to the implementation by means of low cost or better class microcontroller available in the mixed-signal system. Finally, the obtained system self-testing capability makes it possible to investigate its condition during the life cycle and improves system reliability. The detailed information about the proposed testing methodology is placed in Section 2, then, in Section 3, an evolutionary optimization adapted to searching for test desired for specific performance parameters of CUT identification is presented in detail. Finally, in Section 4, there is a description of results of exemplary AECs specification testing by means of the proposed approach together with accuracy analysis and performances comparison to the alternative methods. Besides, the evaluation of quantization noise influence to the proposed method preciseness may be found there.

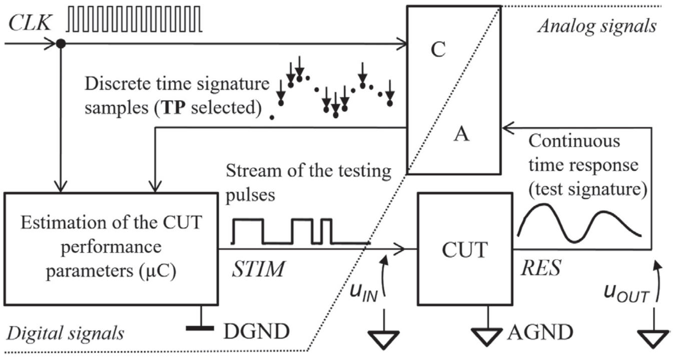

Fig. 1. The proposed system for analog CUT specification testing

2. Specification testing method description

The aim of the proposed method is the correctness verification of the I selected analog circuit under test (CUT) performance parameters from the assumed set **P**:

$$\mathbf{P} = \left\{p_0, p_1, \ldots, p_{(I-1)}\right\}. \tag{1}$$

It should be emphasized that the described AECs testing technique has been designed to the final product specification requirements verification and it involves the necessity of the possible highest preciseness of (1) estimations assuring. This assumption is especially important in the areas of acceptable levels of the CUT performance parameters (i.e., in their tolerance regions). The maximal identification error and its standard deviation minimization are crucial for the method and have to be especially optimal in the ranges of (1) guaranteed by the producer. Finally, if one or more performance parameters exceed product specification, then the CUT is classified as a faulty one or is respectively sorted to the group of worse quality products (e.g., offered with a reduced price). This testing concept gives great approach to the AECs production yield maximization and its permanent controlling. Of course, the final electronic products which have to be highly fail-safe during all their life cycle (e.g., medical, automotive or environment monitoring ones) may be easily tested at the user stage in the proposed way too.

2.1. Specification testing idea. For the proposed solution, the actual levels of (1) are determined by means of the quick test procedure illustrated in Fig. 1. During the testing stage the CUT is excited by the specialized signal *STIM* constructed from D digital pulses with rising and falling edges placed at the defined time moments (exact numbers of *CLK* periods):

$$\mathbf{STIM}_i = \left\{n_{Hi0}, n_{Li0}, n_{Hi1}, n_{Li1}, \ldots, n_{LiD}, n_{LiD}\right\}, \tag{2}$$

for which distribution was optimized to i-th performance parameter identification by means of evolutionary computations in the way explained in Section 3. This stream of digital pulses may be easily generated from a low-cost digital circuit output without the necessity of using a D/A converter. Besides, this kind of stimulus assures a rich frequency spectrum of CUT excitation and may be easily stored with a low cost of implementation – it takes very small area of FLASH memory of mixed-signal electronic systems defining a digital pulses sequence specialized to the specific performance parameters of the CUT identification. Of course, the digital pulses amplitudes and their slopes have to be stable, repeatable and finally, the applied test sequence generator has to produce testing pattern that is equivalent to the one used during the before test simulation stage. The tilts of pulses edges as well as their amplitudes may be guaranteed by the known performances of specific production technology of digital circuit applied in the tested system (e.g. $t_r = 50$ ns of rise and fall time for TTL standard and typical values of V_{OL}, V_{OH} logical levels) or by use of dedicated signal buffer designed respectively to guarantee the excitation generator with assumed electrical restrictions. Additionally, actual logical voltage levels V_{OL}, V_{OH} of pulses can also be tested and the acquired analog signature may be corrected by respective normalization procedure (under assumption of linear relationship between input signal levels and output response in the specification tolerance area). However, the time synchronization of this testing system is well assured by applying the global clock signal *CLK*. This feature is very important because it guarantees high time accuracy of the excitation synthetizing and samples acquiring processes. In effect, the *STIM* excitation signal (2) edges as well as recorded N probes of response RES:

$$\mathbf{RES}_i = \left\{v_{i1}, v_{i2}, \ldots, v_{iN}\right\} \tag{3}$$

of analog signature are placed in exact points of time with an accuracy precisely defined by CLK tact period T_{CLK} in the way explained in Fig. 2. These exemplary oscillograms represent some hypothetical signals from the test system proposed in this work. As may be seen, the places of positive edges of *STIM* signal pulses, the time moments of analog signature *RES* probes are defined univocally by the *CLK* periods synchronizing this system. During completing the digitalized signature, the test points tp_1, tp_2, …, tp_8 discrete levels may be precisely determined by the A/D converter clocking from global *CLK* and finally they are gathered to the CUT diagnosing purpose. The digital excitation *STIM* (2) pulses density and the J test point

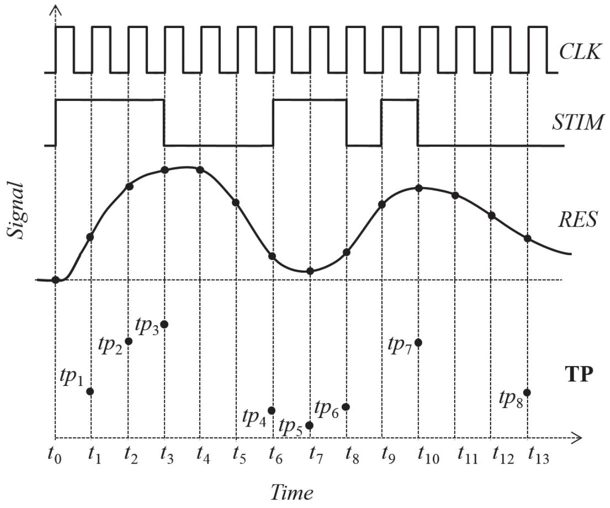

Fig. 2. The exemplary waveforms for the proposed testing system

locations (the selected probes indexes $\langle 1,\ldots,N\rangle$ of digitalized response *RES*):

$$\mathbf{J}_i = \{n_{i1},\ldots,n_{iJ}\} \tag{4}$$

are optimized in the evolutionary system and after the testing measure stage finalization, the set of input variables:

$$\mathbf{TP}_i = \{tp_{i1}, tp_{i2},\ldots,tp_{iJ}\} \tag{5}$$

is ready to the i-th performance parameter actual level identification. When set (3) is collected, the acquired probes are arguments of the modified mathematical regression model formula:

$$\begin{aligned}\hat{p}_i = \beta_{i0} &+ \\ &\beta_{i1} median\left[\mathbf{V}\left(\frac{n-n_{i1}}{W}\right)\right]^{k_{i1}} + \\ &\beta_{i2} median\left[\mathbf{V}\left(\frac{n-n_{i2}}{W}\right)\right]^{k_{i2}} + \\ &\vdots \\ &\beta_{i(J-1)} median\left[\mathbf{V}\left(\frac{n-n_{i(J-1)}}{W}\right)\right]^{k_{i(J-1)}} + \\ &\beta_{iJ} median\left[\mathbf{V}\left(\frac{n-n_{iJ}}{W}\right)\right]^{k_{iJ}}\end{aligned}, \tag{6}$$

where i is the identifier of the tested parameter (explained variable), n_{ij} are test points (5) probes indexes from (4) and k_{ij} denotes power coefficient $\pm\langle 1,\ldots,K\rangle$ of non-linear transformation of acquired signal sample digitized value (power of term from estimation formula):

$$\mathbf{K}_i = \{k_{i1},\ldots,k_{iJ}\}. \tag{7}$$

This implemented possibility of the above regression model arguments recalculation with negative or positive power up to K creates general nonlinear estimation model with variables preprocessing that may be optimized for explaining the identified performance parameter selected from (1). Additionally, the proposed mathematical model arguments:

$$\lambda_{ij} = median\left[\mathbf{V}\left(\frac{n-n_{ij}}{W}\right)\right] \tag{8}$$

are nonlinearly filtered in median filter with input data set obtained from rectangle window of W probes concentrated around the n_{ij} test point respectively (4). This median filter assures the resistance of the method to the measure noises for very low additional cost of implementation. Especially, it rejects amplitude, high energetic noises which may propagate in the mixed-signal system paths and disturb analog values of the test signature. After finalizing the described acquiring and preprocessing steps, the regression function explanatory variables are:

$$\mathbf{X}_i = \left[\ (\lambda_{i1})^{k_{i1}},\quad (\lambda_{i2})^{k_{i2}},\quad \ldots,\quad (\lambda_{iJ})^{k_{iJ}}\ \right], \tag{9}$$

which creates the J element vector of variables from the formula (6) terms:

$$\mathbf{X}_i = [x_{i1},\ x_{i2},\ \ldots,\ x_{iJ}]. \tag{10}$$

However, the model real numbered parts of terms β_{ij} create coefficients vector:

$$\boldsymbol{\beta}_i = \left[\ \beta_{ij_0},\quad \beta_{ij_1},\quad \ldots,\quad \beta_{ij_J}\ \right], \tag{11}$$

that is determined by means of multiple regression procedure [28] and it defines adequately the relation between preprocessed arguments (10) and the specific i-th tested performance parameter of the CUT:

$$\hat{p}_i = \boldsymbol{\beta}_i \cdot \left[1,\ \mathbf{X}_i\right]^T. \tag{12}$$

These regression coefficients (11) are calculated statistically during the test design stage based on $\frac{L}{2}$ subset of random simulation patterns. The standard multiple regression procedure [24, 28] assures the minimal estimation MSEs between the levels of tested performance parameter for CUT, which are known for training set of patterns and the ones estimated by means of regression model (12) with input variables (10) preprocessed previously in the way (9).

As was mentioned, the target structure of the proposed model (6) is determined in the evolutionary system of optimization explained in Section 3. The values from the sets $\mathbf{J}_i$ and $\mathbf{K}_i$ are selected evolutionarily and this process assures searching for the most representative (able to explain the i-th tested parameter) groups of test points selected from (3), the most optimal definition of power factors (7) for preprocessing, nonlinear transformations, as well as for minimized formula (6) size. All the criteria formulated here are included to error fitness function Q_{ERR} of the evolutionary system of optimization. The cyclical computations synthesize the optimal stimulus (2) shape and the mathematical model features mentioned in the same evolutionary system that assures full interaction during searching for the most appropriate design of AEC specification test. The excitation pulses relocations and their widths changes impact directly on estimation formula (6) structure, its elements quantity and coefficients values, and the evolutionary algorithm is trying to find phenotype (digital stimulus and regression model) that finally will be the best evaluated one.

2.2. Before test simulations. The CUT computational analyses stage is a very important part of the test design algorithm; it impacts directly on the final solution effectiveness. The training patterns consist of the one obtained for all the nominal values, exactly defined during the AEC design stage and $(L-1)$ diagnostic states of the CUT transient analyses result with C circuits' parameters (design constants) perturbed. These parameters are independently and randomly dispersed in the assumed range $\pm\delta_{dev}$ around their nominal levels (with uniform probability of randomization procedure). During the computer aided analyzes of $(L-1)$ perturbed CUTs, the values of passive electronic components (e.g., resistances, capacitances, inductances) or/and the sort of specific parameters of active components (e.g., MOSFET transistors channels dimensions, operational amplifiers slew rates, CMMRs) of the simulated AEC are deviated randomly and finally each one takes value from the assumed range:

$$\gamma_d = \gamma_d^{nom}\left(1 \pm \delta_{dev}\right), \tag{13}$$

where $d = \langle 0, \ldots, (C-1) \rangle$ is the index of parameter determination case and nominally $\gamma_0 = \gamma_0^{nom}$. The dispersions (13) of the AEC components parameters directly influence the tested specifications (1) and this procedure results with the L testing (teaching) patterns set creation that is the base of evaluation of the phenotypes considered during the specification test designing stage. During the before test stage the candidates for pulse testing excitations coded in genotypes together with estimation model formulas are tested on the whole training set containing definitions of analyzed CUT teaching cases prepared respectively to the above scenario. The individual from population (genotype containing two chromosomes, i.e., the ones describing testing stimulus and tested performance parameters identification model structure) and coefficients obtained by means of multiple regression strategy define the test stage strategy completely and unequivocally. These coded specification test procedures are evolving among the generations and due to specific form of fitness function and respective reproduction criteria, well fitted, promising ones are spreading over all next populations of the training stage especially. Numerous streams of testing pulses compositions as well as the mathematical identification model structures are explored, successively modified during evolutionary cycles of training stage and adjusted respectively to the coding scheme of leaders. Finally, this before test training results with the best, optimal solution, i.e., the most appropriate definition of specification test encountered during all evolutionary cycles.

As may be easily noticed, the L transient analyses of CUT are necessary for the whole training set determination for each form (2) of pulses stream *STIM* defined in the population of G_{MX} solutions (phenotypes). It means that totally $L \cdot G_{MX} \cdot I_{MX}$ executions are needed for I_{MX} evolutionary iterations of evolutionary optimization algorithm. Of course, this time-consuming process is started only at the before test stage but still it is quite a strict and uncomfortable requirement that in the proposed procedure was omitted in the way that resulted from the nature of the considered specification driven testing of the linear AECs. The aim of the technique is a precise estimation of the diagnosed performance parameters of the CUT and especially the resulted mathematical model (6) has to be possibly most accurate around the nominal area defined by (13), where the GO/NO-GO diagnostic threshold criteria are placed. It means that the analog diagnostic signature (3) for any considered complex stimulus (2) may be determined as the respective superposition of the $2 \cdot D$ step responses $h_e(m)$ shifted to the discrete time points $n_{Hid} \cdot T_{CLK}$, $n_{Lid} \cdot T_{CLK}$ of the specialized excitation rising and falling edges respectively:

$$\mathbf{RES}_i = \sum_{r=1}^{2D} f_a(r) h_e(m - n_r), \tag{14}$$

where $f_a(r)$ is an activation function of the r-th component that returns ± 1 after rising or falling edge component detection in n_r points of digital stimulus. The described simplification effects with the number of AEC external simulation program .TRAN analyses reduction to L ones only, i.e. the natural responses $h_e(m)$ of all the training circuits cases are only L times calculated in simulation software initially. Next, for all the other pulses (2) distributions (pulses combinations) evaluated during evolutionary cycles, the test signature responses (3) are determined by the use of the above superposition rule. This special feature effected with radical reduction of the before test time cost of the test design stage and allowed to make more numbers of evolutionary optimization cycles in the acceptable time of before test stage procedure.

3. Evolutionary computations

The optimal binary code of stimulus $\mathbf{STIM}_i$ as well as test points $\mathbf{J}_i$ and preprocessing coefficients $\mathbf{K}_i$ are searched in the dedicated evolutionary system. The algorithm steps are presented in Fig. 3. Generally, it consists of the three procedural stages: the initial-, the main-, the final-one and the four program loops located in the main part of the optimization software implemented in the MATLAB environment. Fig. 3a illustrates the general overview of the proposed evolutionary optimization system. During the initial stage, the respective parameters (see Section 4) of the EA system have to be assumed and next, after starting the evolution, the primary initial population is created randomly (i.e., **CH1** and **CH2** genes are set randomly to the allowed alleles values). The signature response obtained to the testing excitations coded in evaluated individual from population is calculated at the beginning of the main algorithm loops part. It allows to determine the set of response samples which are candidates to the test points set optimized evolutionarily together with the regression model coefficients in the secondary EA built in the preliminary one. This inner EA works on **CH2** chromosomes only and it is searching for the optimal mathe-

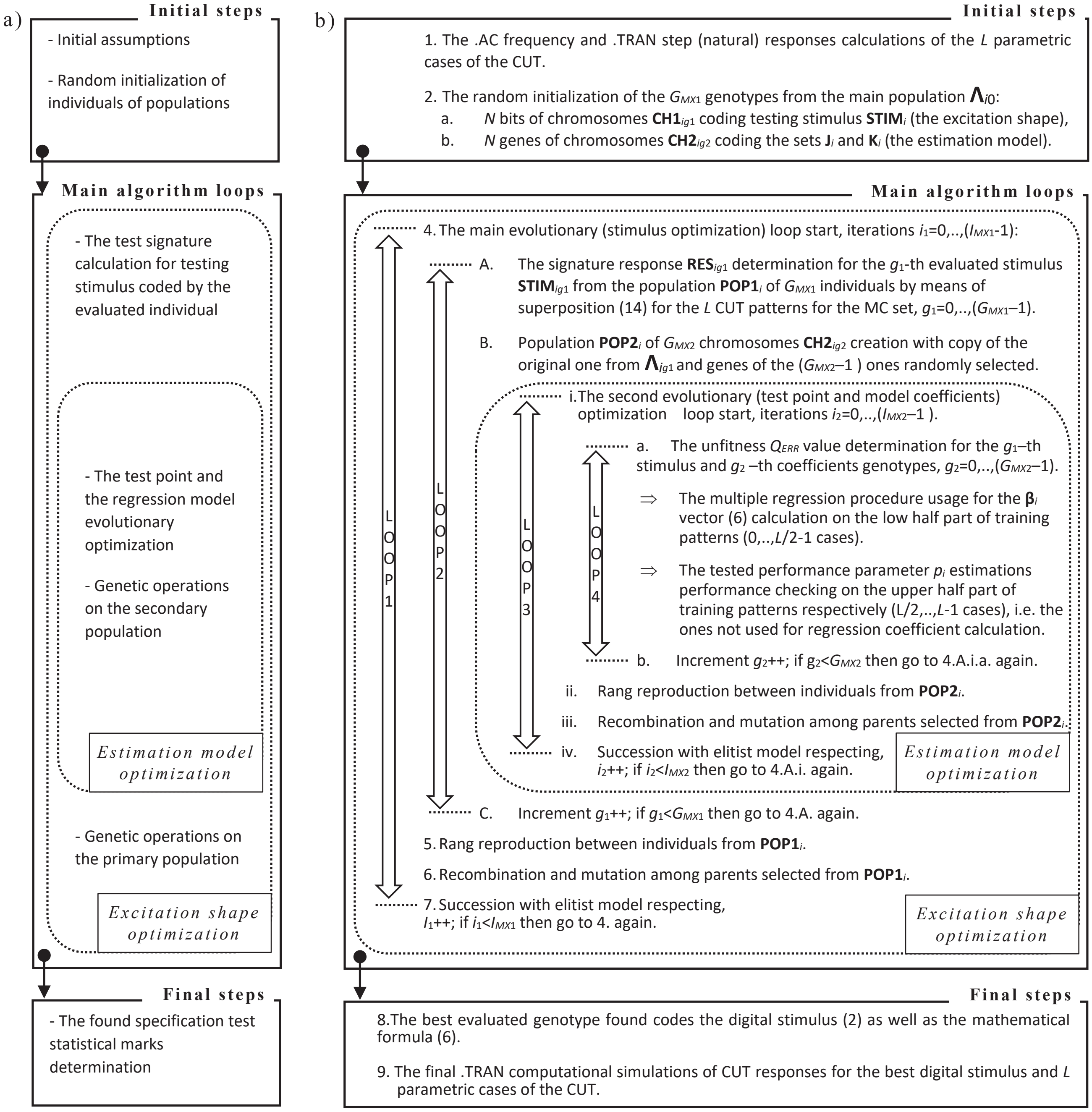

Fig. 3. The evolutionary optimisation algorithm steps: a) general overview, b) detailed diagram

matical model (6) structure among G_{MX2} individuals per cycle of candidates from genetic population. Fitness function of each individual is determined and the best suited (to the currently considered test stimulus shape) is finally selected. After finalizing the I_{MX2} iterations of this evolutionary subsystem, the main loop is continued for the evolutionary operations on **CH1** part of genotype and it assures the testing stimulus shape optimization. These steps described here are repeated G_{MX1} times, i.e., for each genotype from the main generation and finally this process is continued until I_{MX1} generation is reached. At the end, the best evaluated pair of **CH1** and **CH2** codes phenotypes defining the desired specification test of AEC.

As can be seen in a detailed algorithm diagram in Fig. 3b, during the initial part, i.e., just after this system starting, external simulation software tool is executed to determine the frequency and the natural responses for the L random parametric states of the analog CUT. As was explained in the previous section, these Monte-Carlo (MC) simulations are made with the selected CUT parameters perturbed in the assumed areas (13). Besides, the preliminary population of individuals:

$$\mathbf{POP}_i = \left\{\boldsymbol{\Lambda}_{i0},\ \boldsymbol{\Lambda}_{i1},\ \ldots,\ \boldsymbol{\Lambda}_{i(GMX1-1)}\right\} \tag{15}$$

is randomly created during this introductory stage.

Each genotype $\mathbf{\Lambda}_{ig}$ above consists of binary chromosome $\mathbf{CH1}_{ig1}$ coding stimulus stream (2) and integer one $\mathbf{CH2}_{ig2}$ with factors defining the estimating formula (6) structure:

$$\mathbf{\Lambda}_{ig} = \left\{ \mathbf{CH1}_{ig1},\ \mathbf{CH2}_{ig2} \right\}. \tag{16}$$

As may be seen in Fig. 4, the chromosome $\mathbf{CH1}_{ig1}$ alleles are binary 0 or 1 values directly coding the logical state of the digital test stimulus during the specific system clock tact period T_{CLK}. However, the genes of $\mathbf{CH2}_{ig2}$ reach integer numbers from the allowed alleles set $\langle 0, \dots, 2K \rangle$ and in case of non-zeroed one the specific sample point (i.e., synchronized by T_{CLK} sampling period to the gene location) is selected as a testing point with the value of power factor of nonlinear preprocessing recalculation in model (6) coded by the positive integer number (i.e., this gene position index and code value respectively decoded to $\mathbf{J}_i$ and $\mathbf{K}_i$). Otherwise, for the zeroed n-th gene of $\mathbf{CH2}_{ig2}$, the test point (the sample of response signature (3) acquired on n-th test measure cycle) is rejected (as explained in Table 1). This hybrid structure of genotype allows to optimize different features of the phenotype concurrently in the same system.

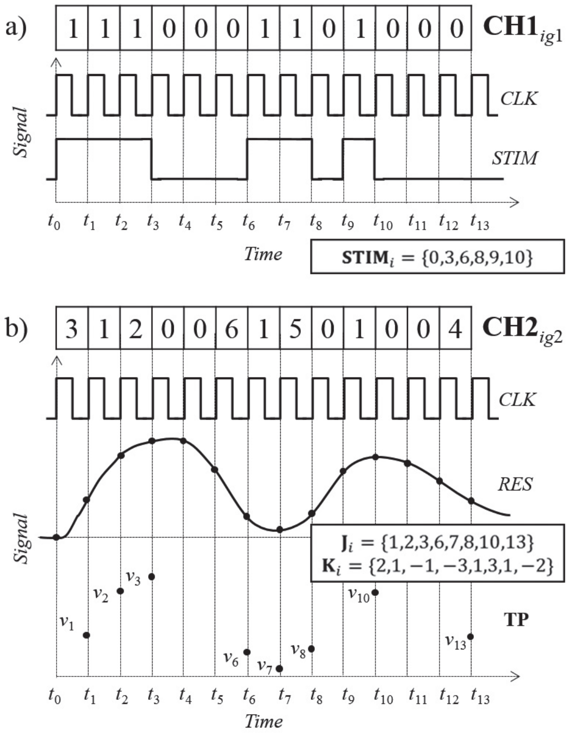

Fig. 4. The exemplary chromosomes and phenotypes: a) of digital stimulus, b) of estimating formula model

When preliminary population is ready, the main algorithm begins and generally it consists of the two evolutionary systems which are tied together. The 1-st and 2-nd program loops define the main evolution part that impacts stimulus shape chromosomes $\mathbf{CH1}_{ig}$, however the 3-rd and 4-th loops cover the evolutionary optimization section that is searching for the chromosome best suitable to the currently analyzed stimulus pulses decomposition in population of individuals $\mathbf{CH2}_{ig}$.

Table 1
Chromosome CH2 genes interpretation

Gene		Interpretation result
Position	Code	
t_n	0	Reject n-th test point.
	1	Use $(v_n)^1$ direct n-th signature sample.
	2	Use $(v_n)^{-1}$ inverted n-th signature sample.
	3	Use $(v_n)^2$ preprocessed n-th signature sample.
	4	Use $(v_n)^{-2}$ preprocessed n-th signature sample.
	5	Use $(v_n)^3$ preprocessed n-th signature sample.
	6	Use $(v_n)^{-3}$ preprocessed n-th signature sample.

The 1-st loop of the main algorithm iterates I_{MX1} times of global generations of $\mathbf{POP}_i$. Each specific binary testing stream from population $\mathbf{POP1}_i$ of G_{MX1} individuals:

$$\mathbf{POP1}_i = \left\{ \mathbf{CH1}_{i0},\ \mathbf{CH1}_{i1},\ \dots,\ \mathbf{CH1}_{i(GMX1-1)} \right\} \tag{17}$$

is evaluated every main loop cycle. All these iterations are defined by 2-nd loop of algorithm. Firstly, the transient response signatures $\mathbf{RES}_{ig}$ are determined by composition (14) for all the L teaching patterns and the g_1-th stimulus chromosome ($g_1 = 0, \dots, G_{MX1} - 1$) from (17). This step allows to obtain the full training set of test signatures digitalized probes (3) available to the identified performance parameter of the CUT estimation. Next, the second evolution begins and along I_{MX2} iterations of 3^{rd} loop the optimal test point indexes $\mathbf{J}_i$ (4) as well as the model parameters $\mathbf{K}_i$ (7) are searched for among G_{MX2} of $\mathbf{POP2}_i$ individuals. Initially, the second preliminary generation of the evolutionary subsystem is created:

$$\mathbf{POP2}_i = \left\{ \mathbf{CH2}_{i0},\ \mathbf{CH2}_{i1},\ \dots,\ \mathbf{CH2}_{i(GMX2-1)} \right\} \tag{18}$$

and it consists of the original copy of chromosome $\mathbf{CH2}_{ig1}$ from (15) and the $(G_{MX2} - 1)$ randomly created ones. Next, during the 4-th loop cycles, the error fitness factor Q_{ERR} is calculated for the g_1-th stimulus signal chromosome from (17) and for each combination of the estimation model structure defining genes (18). During the reproduction procedures of these both evolutionary parts, the individuals from $\mathbf{POP1}_i$ as well as from $\mathbf{POP2}_i$ with better quality factor (a lower value of Q_{ERR}) are promoted and it results with a higher probability of their reproduction to the mating pools, more frequent genetic crossover and the new offspring genotype chains creation in result respectively.

The detailed description of the phenotype fitness determination procedure and genetic operations schemes are placed in the next subsections, but computational consequence of the proposed algorithm execution is the genotype Λ_{iBEST} designing that codes the optimized i-th specification test procedure (i.e., the stimulus shape (2) and the model (6) dedicated to the i-th performance parameter of the CUT identification).

Finally, the vectors: $\mathbf{STIM}_i$ consists of $2 \cdot D$ integer numbers (for D digital pulses), $\mathbf{J}_i$, $\mathbf{K}_i$ each with J integer coefficients as well as the real numbered regression coefficients vector $\boldsymbol{\beta}_i$

consists of $(J+1)$ elements (where J denotes the number of test points selected evolutionarily) defines i-th specification test of AEC univocally. It means that for integer and real numbers coded on 2 bytes and 4 bytes (MATLAB single precision or microcontroller system float type variable) respectively, the FLASH memory size (in bytes) needed to single test full definition may be calculated from:

$$SIZ_i = 2\,(2D + 2J) + 4\,(J+1) = 4D + 8J + 1 \tag{19}$$

in bytes respectively. However, the formula for the testing time cost estimation of the i-th identified performance parameter by means of digital stimulus with T_{CLK} period of D_{MX} pulses may be described as:

$$TIM_i = D_{MX} \cdot T_{CLK} + t_{ADD} \cdot (J+1) + (t_{MUL} + t_{SQR}) \cdot J, \tag{20}$$

where t_{ADD}, t_{MUL} and t_{SQR} are times necessary to the floating-point arithmetic addition (about 100 machine cycles of the microcontroller system), multiplication (about 200 cycles) operations and time consumption of the square (for the negative power coefficients) calculations on the integer values of the acquired samples (should not be more than 200 cycles). Equation (20) consists of test stimulating and data processing time parts, i.e., the most absorbing test stage operations. Assuming the method implementation to the chip microcontroller with clock frequency equal to 20 MHz (about 50 µs per 100 machine cycles), the test time cost may be approximately calculated in seconds from:

$$TIM_i = D_{MX} \cdot T_{CLK} + 250^{-6} \cdot J + 50^{-6}. \tag{21}$$

3.1. Fitness error function.

The fitness error proposed to the phenotype quality evaluation consists of the four criteria:

$$Q_{ERR} = \mu_1 \left(1 - R_1^2\right)^2 + \mu_2 \left(1 - R_2^2\right)^2 + \mu_3 \varepsilon_{MX} + \mu_4 \frac{J}{N}, \tag{22}$$

where R_1^2, R_2^2 are determination coefficients (R-squared standard statistical measure of the mathematical model fit correctness) calculated on lower and upper halves of the training patterns set (i.e. this indexed as 1-st represents the model efficiency reached after multiple regression procedure and 2-nd defines the model generalization level), ε_{MX} is the maximal absolute estimation error determined on the whole analyzed set of L patterns and the last section is quotient that represents a normalized size of estimation model (quantity J of the explanatory variables related to the signature response samples set size N). The weights μ_1, μ_2, μ_3, μ_4 denote the priorities of the particular criteria optimization.

3.2. Genetic operations.

During each evolutionary cycle of the described system of optimization the reproduction, the crossover, the mutation and the succession operations are made.

The reproduction is started in steps 5 and 4.B.ii of algorithm from Fig. 3b and the rank method [20–22] was used there. After the fitness mark (22) determination, parent pool gathering procedure is started. Then all the individuals in population are sorted by quality factor in descent order and the index position obtained in this queue (values from 1 up to G_{MX}) denotes rang ρ obtained by genotype. Next, the probability of the individual selection to the mating pool is calculated from:

$$P_{SEL} = P_{MN} + (1 - P_{MN})\,\frac{\rho}{G_{MX}} \tag{23}$$

and the candidates for parents' genotypes set are collected respectively. This kind of reproduction scheme gives the chance of selection for crossover purpose to worse evaluated chromosome chains, it protects against too fast evolutionary convergence to the strongly dominant local extremums of the searching area. It assures better sampling of the possible solutions space. Genetic material recombination is made with probability P_{CR} during the crossover stage on the pairs of individuals randomly chosen from the reproducing pool. As can be seen in Fig. 5, during crossover procedure of parental chromosome pair **CHy** and **CHz**, the crossover points CP_n are selected with random steps successively moving position from the start to the end of code and they define chains cutting points respectively. Next, the dominant, inherited by offspring genotype parts (i.e., expansive genes, y or z in Fig. 5) are selected randomly with equal probability and they create the child chromosome. It means that exchanged genetic material, present in the offspring chain, may be inherited from a mating pair with the same chance and the phenotype features of both parents may spread over the next generations. During the genetic recombination process, the child genes may be mutated with the assumed probability P_{MU} and then they obtain the code selected randomly from the available alleles set.

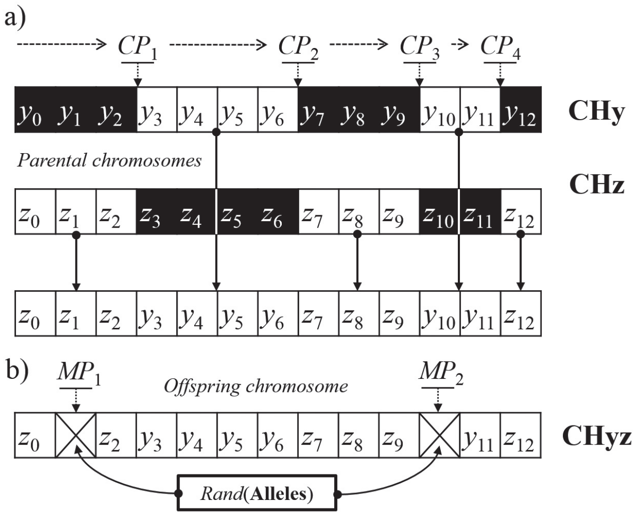

Fig. 5. The schemes of genetic operations: a) crossover, b) mutation

Additionally, to assure the desired selection pressure during reproduction processes and to avoid algorithm stagnation, the phenotypes coding scheme (particular gene positions in chromosome chain) is optimized during evolutionary cycles with the procedure proposed in [23]. This code mapping modification is started every time before recombination, and it is defined by placement of a non-zeroed genes of the current best individual (leader over all the generations). All its set genes are moved to the common section ("glued together" with their original positional phenotype interpretation preservation), next all the other genotypes from population are coded in the same way. This simple technique results with span of coding scheme minimization of well fitted phenotypes and this partially protects them before cutting during crossover stage.

4. Example circuits specification testing

This section presents statistical effectiveness of testing results obtained to the CUTs proposed as benchmark in the papers published previously [24, 26, 29–33]. The evolutionary system was started individually for each considered example CUT but with the same initial parameters described in Table 2.

Table 2
The evolutionary system of test design initial settings

Notation	System parameter description	Value
L	The MC training set size	200
D_{MX}	The maximal number of testing pulses	48
K	The range of the model formula power factors	3
G_{MX1}	The size of main population	20
G_{MX2}	The size of secondary population	20
I_{MX1}	The number of main generation iterations	60
I_{MX2}	The number of secondary generation iterations	50
P_{CR}	The crossover operation probability	0.9
P_{MU}	The mutation operation probability	0.2
W	The median filter window sample width	5
μ_1	The weight of standard regression model quality	0.1
μ_2	The weight of model generalization efficiency	1
μ_3	The weight of maximal estimation error impact	0.1
μ_4	The weight of model size minimization	0.001

Initial values of parameters have been determined experimentally for the presented examples. Their definition is a compromise among before test calculation time, final size of mathematical estimation model and its inaccuracy. Of course, adjusting initial settings of analog specification test design involves the additional experimental executions of the evolutionary iterations, but the general properties for the specific settings are known and it made this process much easier. The evolutionary generations sizes G_{MX1}, G_{MX2} and the numbers of iterations I_{MX1}, I_{MX2} should be possibly large but they directly impact on the before test calculation time. The values proposed in Table 2 assured a good performance of the results obtained with the standard quad-core PC with 3.2 GHz clock. In practice, these settings just may be enlarged respectively to the available higher performance of the professional workstation. Similarly, the training patterns set size L should be as high as possible, however for the considered examples the L was limited to the same quantity as assumed for the competitive referenced methods. Crossover and mutation probabilities define the efficiency of the searching space sampling and generally, for assuring the respective expansion of coding schemes of well fitted individuals and for obtaining the searching space effective probing, the crossover probability P_{CR} should be quite high (near to 1) and significantly more than mutation operation P_{MU} (near to 0.1), i.e., as it is typical for the evolutionary optimization systems. The local regulations of these probability settings do not affect noticeably the performance of the proposed method. The mathematical formula power factors range K and the number of testing pulses D_{MX} should be chosen as a compromise between test cost (time) and its accuracy. The values proposed in Table 2 assured model terms with enough power factors range and enough test stimulus length available during the model composition and this was confirmed by the high-quality estimation results. The weights $\mu_1, \ldots, \mu_4$ of the four criteria of fitness function components have been assumed to obtain the highest priority for the estimation model generalization capability optimization (processed on the second half part of training patterns). Next, optimization criteria are considered with the decreasing order of priority levels respectively: the maximal estimation error minimization, the determination coefficient maximization (multiple regression processed on the first half of training set) and the model size with the lowest priority. The following weights values proposed in Table 2 are obtained by dividing the previous ones by 10 and it guarantees that the following criteria cannot mask the previous one stronger than 10% of its current level. The median filter window width W may be determined by means of measure noises expected in the tested analog system analysis and it rejects the amplitude pulse distortions which time duration is less than half of time width of this window.

4.1. Low-pass leap-frog filter. The first example AEC assumed to the specification correctness verification is the low pass 4-th order filter presented in Fig. 6. The below CUT pa-

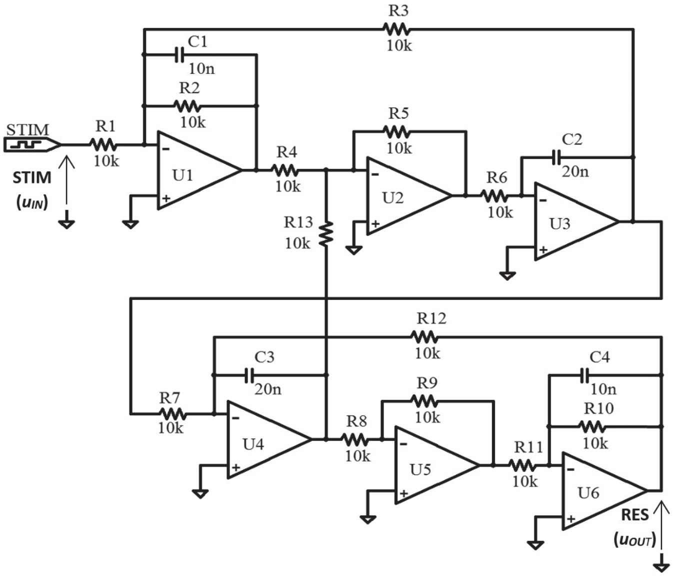

Fig. 6. The example leap-frog filter CUT benchmark [29, 30]

rameters were selected to the diagnostic identification:

$$\mathbf{P} = \{|K_{DC}|,\ |K_{MX}|,\ f_{-3dB},\ f_{-20dB},\ \varphi_{-3dB},\ \varphi_{-20dB}\} \quad (24)$$

and there are: DC and maximal gains, frequencies and signal phase shifts at −3 dB and −20 dB attenuations points respectively. The assumed test system clock frequency $f_{CLK} =$ 20 kHz, i.e., more than 10 times of the filter −3 dB corner frequency. During the training patterns set creation stage, the $L = 200$ diagnostic states of the CUT were analyzed (i.e., with the 100 random cases for regression model calculation as well as 100 ones for its generalization effectiveness checking purposes). The evolutionary system of optimization was started for each specification (24) independently and Table 3 presents determination coefficients, calculation times, and model parameters respectively obtained for the best phenotypes found. “Est. testing time” in Table 3 is the approximate duration time of the test procedure calculated from (21), i.e., under assumption of this specification test implementation to microcontroller with 20 MHz clock. This time consists of periods necessary to the CUT excitation generation and the acquired data processing.

Table 3
The found best phenotypes quality marks and costs

	Coefficients of determination		Model costs representing parameters			
	Reg. patterns (R_1^2)	Gen. patterns (R_2^2)	Before test opt. time [min.]	No. of test points (J)	Model desc. Size [Bytes]	Est. testing time [ms]
$\lvert K_{DC}\rvert$	1.0000	1.0000	70.0	4	137	3.45
$\lvert K_{MX}\rvert$	0.9986	0.9992	77.1	9	153	4.70
f_{-3dB}	0.9994	0.9994	76.5	15	221	6.20
f_{-20dB}	0.9999	0.9998	71.5	10	157	4.95
φ_{-3dB}	0.9983	0.9969	83.0	24	289	8.45
φ_{-20dB}	0.9995	0.9992	74.9	14	221	5.95
Full test cost levels:			**465.2**	**80**	**1178**	**34.7**

The nominal levels of all tested parameters, their deviations caused by $\delta_{tol} = 5\%$ of normally distributed tolerance dispersion of the values of all discrete elements and the accuracies of the phenotypes found evolutionarily for patterns set form MC analysis of cases randomized with uniform probability and $\delta_{dev} = 10\%$ deviation are shown in Table 4.

Next, the estimation models’ generalization capabilities were checked on the 100 newly created random patterns for δ_{dev} =5%. In the identical way the method previously proposed in the work [24] was statistically verified. For both techniques only the output signal shape is analyzed at the specification test stage. However, for the previous approach the test response is a natural one (only to the single step stimulus), but the newly proposed method uses a stream of pulses as testing excitation for that decomposition is optimized evolutionarily to the specific performance parameter identification. The structures of genotypes are completely different for these two methods (i.e., genotype tree vs string chromosomes).

Table 4
The training set patterns identification accuracies

	Design specification		Estimation model quality			
			Identification error (for δ_{dev})			
	Nom. level	Allowed abs. dev. (for δ_{tol})	Avg. level [%]	Max. level [%]	Std. dev. [%]	Fit. value Q·10^3 [mili]
$\lvert K_{DC}\rvert$	0.5	0.15	0.017	0.072	0.013	0.141
$\lvert K_{MX}\rvert$	0.5	0.15	0.261	1.471	0.231	0.946
f_{-3dB} [Hz]	1462	207	0.119	0.438	0.093	0.701
f_{-20dB} [Hz]	2446	259	0.043	0.164	0.034	0.373
φ_{-3dB} [deg]	165.9	14.6	0.142	0.723	0.121	1.233
φ_{-20dB} [deg]	81.2	11.3	0.091	0.307	0.068	0.599
Averagely (for $\delta_{dev} = 10\%$):			**0.112**	**0.529**	**0.093**	**0.666**

The comparison of the mathematical model final accuracies of these two alternative approaches may be seen in Table 5. The preciseness achieved by the technique proposed is significantly higher than for the one published previously. The test stimulus individually specialized to the specific performance parameters investigations effects with major improvement of the multiple regression formula estimations effectiveness. The determination coefficients (see Table 3) for the training pattern sets are very near to 1 that means excellent mathematical model fitness to the considered problem and generalized effectiveness presented in Table 5 proved it. The CUT total testing time estimated for the considered method is close to 35 ms, so it takes about 20 ms longer than for the referenced one. However, this small difference may be accepted in practice, especially because of the analog test reliability satisfactory improvement. Of course, the before test computational effort necessary dur-

Table 5
The proposed method performances comparision to the referenced one

	Proposed method			Referenced method		
	Avg. level [%]	Max. level [%]	Std. dev. [%]	Avg. level [%]	Max. level [%]	Std. dev. [%]
$\lvert K_{DC}\rvert$	0.018	0.048	0.012	0.063	0.203	0.080
$\lvert K_{MX}\rvert$	0.196	0.594	0.125	0.420	1.444	0.476
f_{-3dB}	0.098	0.329	0.069	0.297	1.074	0.387
f_{-20dB}	0.028	0.092	0.018	0.157	0.657	0.199
φ_{-3dB}	0.090	0.310	0.071	0.600	2.319	0.761
φ_{-20dB}	0.067	0.171	0.045	0.864	3.423	1.115
Averagely:	**0.083**	**0.257**	**0.057**	**0.400**	**1.520**	**0.503**

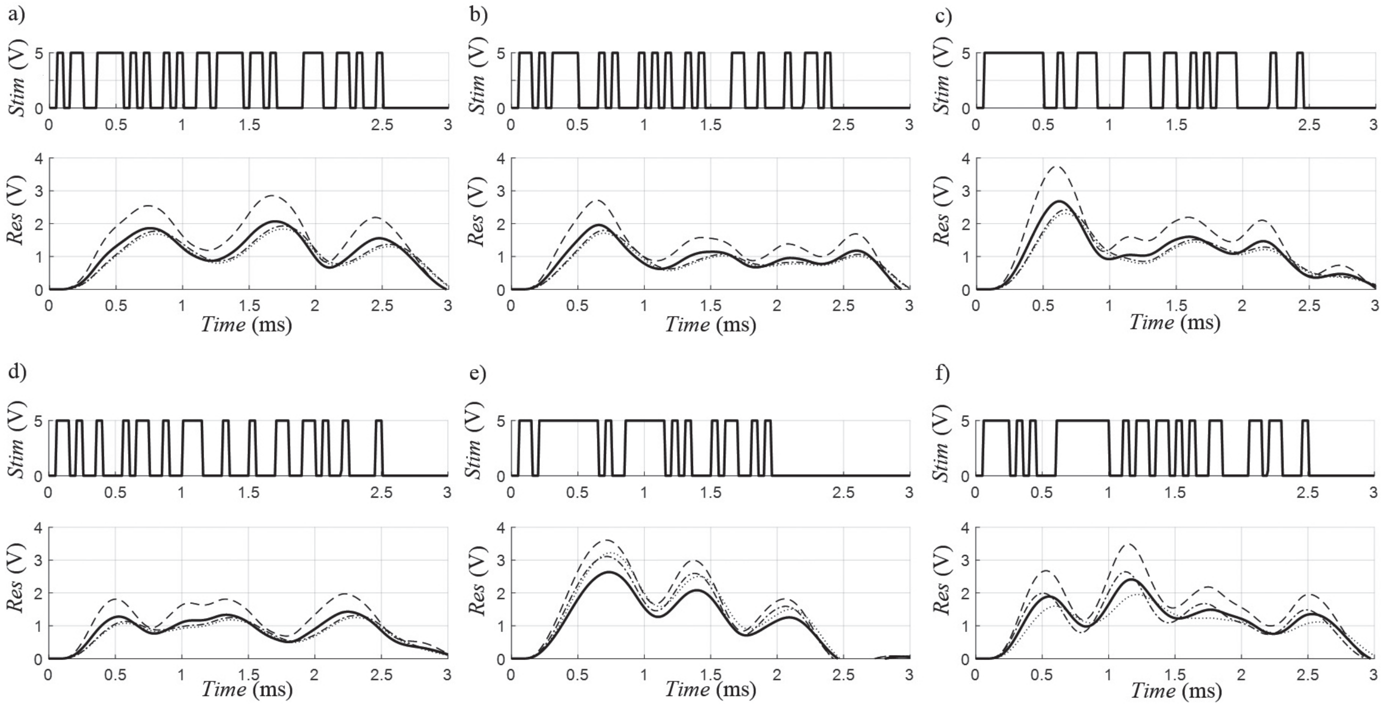

Fig. 7. The evolutionary optimized testing streams of digital pulses and analog diagnostic signatures of CUT nominal state (bold curve) and three other ones obtained for: a) $|K_{DC}|$, b) $|K_{MX}|$, c) f_{-3dB}, d) f_{-20dB}, e) φ_{-3dB}, f) φ_{-20dB} performance parameters tests

ing the design stage is higher about 3.68 times in comparison to the previous solution, but this effort is needed only once and is still acceptable and it is worth to assure this quite good progress of the specification test quality.

All the genotype chromosomes **CH1** which code the digital excitations (presented in Fig. 7) specialized to the assumed specification parameters testing as well as chromosomes **CH2** describing the mathematical regression formulas (6) dedicated to the particular estimations are collected in Table 6. The "three others" example responses cases plotted in Fig. 7 are signature responses found in MC training set for which the maximal absolute momentary deviations are the highest ones (in contrary to the nominal waveform). They show the signature response sensitivity to the CUT elements parameters dispersion.

The binary chromosomes **CH1** presented in Table 6 code the pulses waveforms starting from the second slope from the left side of signal given in Fig. 7, i.e., the first byte of all the excitations is 1 for each case (means the preliminary transition from the initial low-level state to the high one). In other words, the first bit for all digital excitations is always 1 (start bit) and it has not been coded in the genotypes. For example, the beginning of a digital stream found to the $|K_{DC}|$ testing purpose is **CH1** $= 0110011110$ (Table 6) and as mentioned, starting bit is 1 (always set first on t_0 clock cycle start), however the next part of the stimulus is coded by **CH1** string directly. It means that for digital stimulus from Fig. 7a is state 0 during t_1 cycle, next during t_2 and t_3 periods there is 1 (second pulse with 2 system clock period duration). Next, low level is kept during the two cycles and four set bits result with 4 system clocks pulse, etc. Besides, as can be noticed in Table 6, many of the testing points coded in **CH2** are zeroed, so the analog test calculation effort was minimized well. The full, detailed definitions of the designed specification tests are collected in sets (25)–(30) respectively. Table 3, column 5 presents only the quantities of the test points selected, however, their exact time points have been determined evolutionarily and are coded by positions of non-zeroed genes of chromosomes **CH2** respectively. For example, in Table 3 it may be seen that $J = 4$ test points are used to $|K_{DC}|$ estimation and respectively to Table 6 these points are 1, 26, 29 and 36 samples of signature waveform (i.e. set $\mathbf{J}_0$

Table 6
The chromosomes from the best genotypes found

		Best found genotypes
$\lvert K_{DC}\rvert$	CH1	011001111010100101001101111011010000111001101001
	CH2	100000000000000000000000010010000001000000000000
$\lvert K_{MX}\rvert$	CH1	101011110001010001010100101000011001000100110100
	CH2	311010100004000030000500000000000000020000000000
f_{-3dB}	CH1	111111110010011100001111001100101011100000100010
	CH2	060000201200204000003000001005000010100600014500
f_{-20dB}	CH1	101001000101100100111000100010001100110100100001
	CH2	021200000000004000000020000000100000000036001002
φ_{-3dB}	CH1	101111111111010011111101010001011001010000000000
	CH2	105116031066200060012346100056005050050000006005
φ_{-20dB}	CH1	111010100011111111001011011010100110000110110001
	CH2	123025101010000100000205400000100000000000010000

of $|K_{DC}|$ test definition (25)). It means that test points are precisely defined as optimally determined samples of test response signature.

$$\begin{aligned}
\mathbf{STIM}_0 &= \left\{ \begin{matrix} 0,1,2,4,6,10,11,12,13,14,16,17,18,19,21, \\ 23,24,28,29,31,32,33,37,40,42,45,46,48 \end{matrix} \right\}, \\
\mathbf{J}_0 &= \{1,26,29,36\}, \\
\mathbf{K}_0 &= \{1,1,1,1\}, \\
\boldsymbol{\beta}_0 &= \begin{bmatrix} -1.6683142e-4, \\ 4.4135137,\ 0.17878695, \\ 0.013779832,\ 0.15999790 \end{bmatrix};
\end{aligned} \tag{25}$$

$$\begin{aligned}
\mathbf{STIM}_1 &= \left\{ \begin{matrix} 0,2,3,4,5,9,12,13,14,15,18,19,20,21,22,23, \\ 25,26,27,28,32,34,36,37,40,41,43,45,46,47 \end{matrix} \right\}, \\
\mathbf{J}_1 &= \{1,2,3,5,7,12,17,22,38\}, \\
\mathbf{K}_1 &= \{3,1,1,1,1,4,3,5,2\}, \\
\boldsymbol{\beta}_1 &= \begin{bmatrix} 0.26474345, \\ 18699.785,-3.7068841,5.1289968, \\ -2.8482714,1.1403879,-0.11267280, \\ 0.039660078,0.063929446,-0.021744564 \end{bmatrix};
\end{aligned} \tag{26}$$

$$\begin{aligned}
\mathbf{STIM}_2 &= \left\{ \begin{matrix} 0,9,11,12,14,17,21,25,27,29, \\ 31,32,33,34,35,38,43,44,47,48 \end{matrix} \right\}, \\
\mathbf{J}_2 &= \{2,7,9,10,13,15,20,26,29,34,36,39,44,45,46\}, \\
\mathbf{K}_2 &= \{6,2,1,2,2,4,3,1,5,1,1,6,1,4,5\}, \\
\boldsymbol{\beta}_2 &= \begin{bmatrix} -612.23248, \\ -3.6599106e-4,5431.8232,267.88205, \\ -19275.035,13195.227,-1108.2743,-97.154640, \\ 72.188873,-22.478306,505.20694,-293.55383, \\ 17.879721,128.50809,34.115662,-17.037754 \end{bmatrix};
\end{aligned} \tag{27}$$

$$\begin{aligned}
\mathbf{STIM}_3 &= \left\{ \begin{matrix} 2,3,4,6,7,10,11,12,14,16,17,19,22,25, \\ 26,29,30,33,35,37,39,40,41,43,44,48 \end{matrix} \right\}, \\
\mathbf{J}_3 &= \{2,3,4,15,23,31,41,42,45,48\}, \\
\mathbf{K}_3 &= \{2,1,2,4,2,1,3,6,1,2\}, \\
\boldsymbol{\beta}_3 &= \begin{bmatrix} 2942.4773, \\ 28.559303,1915.6235,-542.20514,-35.844059, \\ 388.06610,-64.231651,30.740278,149.54230, \\ -300.41580,194.20697 \end{bmatrix};
\end{aligned} \tag{28}$$

$$\begin{aligned}
\mathbf{STIM}_4 &= \left\{ \begin{matrix} 0,2,11,12,13,15,21,22,23,24, \\ 25,28,29,30,32,34,35,36,37 \end{matrix} \right\}, \\
\mathbf{J}_4 &= \left\{ \begin{matrix} 1,3,4,5,6,8,9,11,12,13,17,20,21,22, \\ 23,24,25,29,30,33,35,38,45,48 \end{matrix} \right\}, \\
\mathbf{K}_4 &= \left\{ \begin{matrix} 1,5,1,1,6,3,1,6,6,2,6,1, \\ 2,3,4,6,1,5,6,5,5,5,6,5 \end{matrix} \right\}, \\
\boldsymbol{\beta}_4 &= \begin{bmatrix} 464.47992, \\ -131099.20,-10394.826,3371.6194,-1243.8929, \\ -5.0434980,55.847294,-264.55789,462.47922, \\ -4.9241133,-366.70947,-136.64738,46.189320, \\ 10.216341,41.228153,59.737732,-112.28525, \\ -45.324127,0.088924535,53.937462,-13.852223, \\ -5.0529475,-13.518766,-1.2820020,-353.91147 \end{bmatrix};
\end{aligned} \tag{29}$$

$$\begin{aligned}
\mathbf{STIM}_5 &= \left\{ \begin{matrix} 0,4,5,6,7,8,11,19,21,22,23,25,26,28, \\ 29,30,31,32,34,36,40,42,43,45,48 \end{matrix} \right\}, \\
\mathbf{J}_5 &= \{1,2,3,5,6,7,9,11,16,22,24,25,31,44\}, \\
\mathbf{K}_5 &= \{1,2,3,2,5,1,1,1,1,2,5,4,1,1\}, \\
\boldsymbol{\beta}_5 &= \begin{bmatrix} 41.087093, \\ 46782.449,-1.7795523,-1878.9785,62.163002, \\ 8.6361837,1.3375294,-30.600607,17.105583, \\ 23.057226,-28.797493,-0.20876272, \\ -15.841782,-3.8582404,-8.4836187 \end{bmatrix}.
\end{aligned} \tag{30}$$

The six performance parameters (24) of the considered CUT may be self-validated periodically by means of BIST methodology [33–35] and for the proposed method this test is completely specified by integer and real numbered above coefficients whose implementation takes less than 2 kB of FLASH memory. Besides, the evolutionarily found digital streams of testing pulses are dedicated to the specific performance parameters and quite easy for generation. So, this solution is very suitable for mixed-signal systems and is reachable for low cost of implementation. Exemplary, the proposed test procedure may be started in the controlled equipment every time after it turns on and it will greatly improve this system reliability. Firstly, for the i-th performance parameters testing purpose, the AEC block of the mixed-signal system should be excited by means of the digital stimulus with rising and falling slopes correlated precisely with CLK cycles defined in vector $\mathbf{STIM}_i$. Next, the test points (CUT response voltage samples) have to be acquired exactly on rising edges of $\mathbf{J}_i$ clock periods. These measured samples are arguments of the mathematical formula with the structure (6) that consist of preprocessing indexes $\mathbf{K}_i$ and regression coefficients β_i. Finally, this mathematical regression model allows to accurately estimate the actual level of the tested specification and it makes possible to decide about the CUT condition.

The comparison analysis of the fault coverage level of GO/NO-GO detections between the described technique and the one proposed in [31] is the next statistical experiment discussed in this work. These two methods were used to the considered exemplary CUT from Fig. 6 diagnostic states detections for the same set of: single parametric (soft) $F0, \ldots, F15$ and catastrophic (hard) $F16, \ldots, F25$ faults as well as for $F26, \ldots, F35$ double ones defined in Table 7. The allowed tolerance dispersion of all values of non-faulty discrete elements is equal to $\delta_{tol} = 5\%$. The faults detections coverage achieved for the proposed method and allowed boundary thresholds Δ_{tol} collected in Table 4 are presented in Table 7.

This table contains the GO/NO-GO test results obtained after the proposed method usage to the faults considered in the referenced works detections. It allows to compare the proposed specification driven test efficiency to the fault detection techniques published previously. The estimation models found by means of the proposed approach are used to the performance parameters (24) identification of the diagnostic cases $F0, \ldots, F35$ defined in this table. Each tested case is obtained for the fault condition from the column 2 (e.g. $F0 \rightarrow$ None, $F1 \rightarrow \mathrm{R2} = 20\mathrm{k}$ mean non-faulty and with single parametric fault R2 = 20k circuit from Fig. 6). All the non-faulty discrete elements values are selected randomly from the tolerance dispersion area δ_{tol} with normal distribution of selection probability (i.e., exactly the same conditions were applied as in referenced works). The CUT is classified as faulty if one or more performance parameters (24) exceed "Allowed abs. dev. (for δ_{tol})" levels collected in Table 4. Columns "good" and "faulty" in group "No. of random patterns of CUT" contain real quantities of healthy and faulty patterns obtained after MC simulations, however, in section "No. of correct detections of CUT" there are columns with the same names which present GO/NO-GO detections efficiency assured by the proposed method. Exemplary, for state $F0$ (all the elements with values dispersed randomly with the tolerance δ_{tol}) there were 96 cases for which all the performance parameters (24) have good levels and 4 cases for which deviation is outside the design specification area. The proposed test has detected 95 "good" $F0$ states and 4 "faulty" states correctly (true positive, proper detections) but 1 "good" state was incorrectly classified as faulty (false negative result, erroneous detection). The 3600 probes of the testing signatures were analyzed totally and reached the level of 99.0% proper detections for the considered approach.

This high-quality level test is very close to the competitive solution based on least squares SVM [31] that achieved averagely 99.3 % of correct classifications. However, in contrary to the referenced one, all the hard faults $F16, \ldots, F25$ here were recognized correctly and the test costs are smaller.

It should be noticed that the total number of analog parametric faults is infinite, i.e., due to continuous character of performance parameters of analog circuits. The cases presented in Table 7 are selected examples, proposed in work [31] and considered here again to make the competitive methods reliable comparison analysis possible. On the other hand, it should be emphasized that the proposed specification test is optimized to obtain high generalization capability and the results achieved for the completely newly generated test patterns are very good, which is confirmed by results collected in Table 5 and similarly for the second considered example respectively. Besides, the proposed approach makes it possible to identify real analog levels of performance parameters of the CUT and it may be

Table 7
The GO/NO GO testing results

CUT state		No. of random patterns of CUT:		No. of correct detections of CUT:	
Code	Condition	good	faulty	good	faulty
F	None	96	4	95	4
$F1$	R2 = 20k	0	100	0	100
$F2$	R2 = 5k	0	100	0	100
$F3$	R2 = 15k	31	69	30	64
$F4$	R4 = 20k	15	85	10	85
$F5$	R4 = 5k	3	97	3	97
$F6$	R4 = 15k	79	21	77	20
$F7$	R8 = 20k	22	78	16	77
$F8$	R8 = 5k	4	96	4	95
$F9$	R8 = 15k	81	19	75	19
$F10$	C2 = 30n	7	93	7	90
$F11$	C2 = 10n	0	100	0	100
$F12$	C3 = 30n	4	96	3	96
$F13$	C3 = 10n	0	100	0	100
$F14$	C4 = 20n	8	92	8	91
$F15$	C4 = 5n	0	100	0	100
$F16$	R2 = 100M	0	100	0	100
$F17$	R2 = 1	0	100	0	100
$F18$	R3 = 100M	0	100	0	100
$F19$	R3 = 1	0	100	0	100
$F20$	R8 = 100M	0	100	0	100
$F21$	R8 = 1	0	100	0	100
$F22$	C2 = 100M	0	100	0	100
$F23$	C2 = 1	0	100	0	100
$F24$	C3 = 100M	0	100	0	100
$F25$	C3 = 1	0	100	0	100
$F26$	R2 = 20k, R4 = 20k	12	88	12	88
$F27$	R2 = 5k, R4 = 5k	0	100	0	100
$F28$	R3 = 20k, R4 = 5k	0	100	0	100
$F29$	R3 = 5k, R4 = 5k	0	100	0	100
$F30$	R4 = 15k, R8 = 5k	5	95	4	93
$F31$	R4 = 5k, R8 = 20k	0	100	0	100
$F32$	C2 = 30n, C3 = 30n	0	100	0	100
$F33$	C2 = 10n, C3 = 10n	0	100	0	100
$F34$	C2 = 10n, C4 = 20n	0	100	0	100
$F35$	C2 = 10n, C4 = 5n	0	100	0	100
Totally:		**367**	**3233**	**344**	**3219**
Test reliability:		**99.0%**			

achieved for any values of the AEC elements, i.e., without assumed here limitation to the selected, quantifiable combinations of faulty elements cases.

4.2. Band-pass analog filter. The second analog circuit considered for the proposed method specification testing effectiveness verification is band-pass Deliyannis-Friend filter [24, 26] for which the circuit is presented in Fig. 8. All initial settings of the evolutionary system are collected in Table 2. Due to a very high sensitivity of this circuit specifications to the electronic elements parameters values variations, the set of training patterns was constructed with allowed deviation $\delta_{dev} = 5\%$ maximally. All the values of discrete components at the test design stage were selected during MC $L = 200$ simulations with uniform probability of randomization. However, the allowed specification tolerances for a healthy circuit were assumed on the level $\delta_{tol} = 2\%$ and for the finally tested response signatures the components parameters are dispersed in this area with the normal kind of density of probability distribution. The same conditions for the method effectiveness evaluation were assumed in the previous work [24]. The analog testing system is clocked with frequency $f_{CLK} = 12.5$ kHz, adjusted experimentally, respectively to the considered benchmark CUT bandwidth. The performance parameters selected for identification are:

$$\mathbf{P} = \{|K_{MX}|,\ |K_{400Hz}|,\ |K_{1300Hz}|,\ \Delta f_{BW}\}, \tag{31}$$

where $|K_{MX}|$, $|K_{400Hz}|$, $|K_{1300Hz}|$ are the filter maximal gain, ones reached at the 400 Hz and 1300 Hz frequency points, however f_{BW} is bandwidth denoted between -3 dB attenuation points.

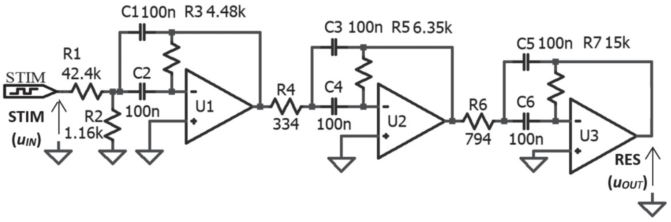

Fig. 8. The example band-pass filter [24, 26]

After finishing the evolutionary computations, the four estimation models with the proposed structure (6) and with $\|\mathbf{J}_1\| = 38$, $\|\mathbf{J}_2\| = 22$, $\|\mathbf{J}_3\| = 21$, $\|\mathbf{J}_4\| = 30$ test points respectively were found. The levels of their determination coefficients are close to 1, each one is higher than 0.99 that confirms the models' excellent matchings. Besides, the four pulse test excitations, which are specialized to the assumed parameters (31) identifications were optimized concurrently in the same evolutionarily system as well. The statistical estimation preciseness achieved for the designed tests are described in Table 8.

The "Allowed abs. dev." in Table 8 is determined statistically by means of MC analysis of 100 random cases for discrete elements parameters dispersed randomly in δ_{tol} tolerance area with uniform distribution of probability (i.e., in the analogical method as for the first example, Table 4). It means an absolute deviation of the tested performance parameter expected (allowed) for the assumed production tolerances of the circuit elements values. As can be seen, the accuracy reached during the training stage is pretty good, better than 2 % for each MC random case. Additionally, low levels of the estimation errors standard deviations prove dominance of precise identifications among statistical probes.

Table 8
The training set patterns identification accuracies

	Design specification		Estimation model quality			
			Identification error (for δ_{dev})			Fit. value $Q{\cdot}10^3$ [mili]
	Nom. level	Allowed abs. dev. (for δ_{tol})	Avg. level [%]	Max. level [%]	Std. dev. [%]	
$\lvert K_{MX}\rvert$	1	0.1	0.528	1.775	0.378	2.484
$\lvert K_{400Hz}\rvert$	0.43	0.05	0.066	0.264	0.058	0.709
$\lvert K_{1300Hz}\rvert$	0.43	0.04	0.036	0.177	0.031	0.615
f_{BW} [Hz]	708	70	0.263	1.268	0.225	1.923
Averagely (for $\delta_{dev} = 5\%$):			**0.223**	**0.871**	**0.173**	**1.433**

Table 9
The proposed method performances comparision to the referenced one

	Proposed method			Referenced method		
	Avg. level [%]	Max. level [%]	Std. dev. [%]	Avg. level [%]	Max. level [%]	Std. dev. [%]
$\lvert K_{MX}\rvert$	0.475	1.513	0.349	1.379	5.679	1.415
$\lvert K_{400Hz}\rvert$	0.044	0.162	0.033	0.188	0.852	0.240
$\lvert K_{1300Hz}\rvert$	0.027	0.103	0.023	0.274	0.929	0.301
f_{BW}	0.230	0.983	0.187	1.112	3.444	1.152
Averagely:	**0.194**	**0.690**	**0.148**	**0.738**	**2.726**	**0.777**

Next, the performance parameters identification accuracy was checked for non-faulty testing patterns pack, generated independently from the training stage and statistical ability of generalization of the approach is shown in Table 9. Besides, there are respective coefficients achieved for the algorithm published earlier in [24]. The quality progress is significant, the accuracies obtained are more than 3 times better in comparison to the ones obtained previously. More complex test stimulus, with optimized distribution of pulses, ensured the specification tests performances improvement. Overall mean identification accuracy index is better than 0.2% and average maximal estimation error is below 1%. Figure 9 presents the decomposition of accurate values of the tested parameters (on X axis) related to the estimated ones (on Y axis), obtained by means of the designed tests. As can be noticed, the values identified lie very near to locations of the best recognitions represented by the diagonal, reference lines. Besides, despite wide variations of the performance parameters occurring in those examined MC sets (maximal dispersions are quite distant from the tolerance boundary levels allowed, defined in Table 8 respectively), the test signature patterns still precisely explain identified values. It proves the method usefulness to the high precise identifications within tolerance area and in the surrounding regions too. The estimation models found represent relations which well determine the observed, verified CUT functional parameters. Generalization capability is satisfying, and the created tests characterize good reliability, the CUT specification passing may be checked efficiently with the minimal cost.

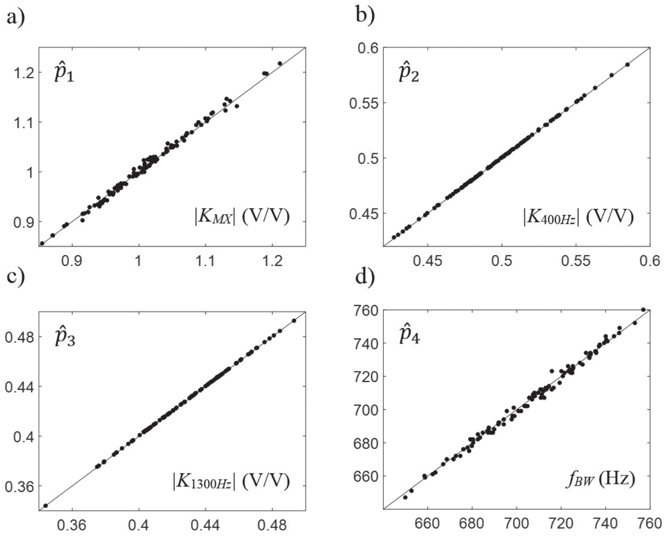

Fig. 9. The exact vs estimated values distributions of: a) $|K_{MX}|$, b) $|K_{400Hz}|$, c) $|K_{1300Hz}|$, d) f_{BW} performance parameters

4.3. Impact of A/D limited resolution. The analysis of impact of the signature quantization on accuracy of the proposed method is discussed in this section. This investigation allows to evaluate the practical usefulness of the technique, when A/D conversion has limited the analog signature resolution before the tested performance parameters estimation process. The preciseness of the identifications models found for the second example CUT was checked again but now this evaluation is made for the different quantization errors (noises) of the A/D conversion. A typical length of the digital code of A/D conversion built in a cheap microcontroller is 12 bits, so the experiment of MC test patterns identifications considered during the second example CUT evaluation was repeated for the A/D with resolution of 12 and 14 bits. All the other conditions are exactly the same as assumed previously during the results collected in Table 9 determination, i.e., only the analog signatures quantization noise is included, and it effects with the identification inaccuracies presented in Table 10.

As can be concluded, the minimal resolution necessary to assure acceptable preciseness of the regression models discussed previously is 14 bits. This kind of A/D conversion allows to obtain identification performances better than for algorithm [24]. However, these results refer to the models trained on the precise (continuous) patterns of diagnostic signatures and it seems to be sensible to try to find the regression formulas optimized to quantized (digitalized) measurements with resolution assumed on the desired level. So, the next experiment considered is the limitation of resolution of training set patterns and evolutionary searching for the estimators adapted to the quantized signatures recognitions. The proposed evolutionary system (Fig. 3) has been started again for resolution of 10 and 12 bits of A/D conversion and the new models (6) have been found with sizes of $\|\mathbf{J}_1\| = 27$, $\|\mathbf{J}_2\| = 23$, $\|\mathbf{J}_3\| = 26$, $\|\mathbf{J}_4\| = 29$ test points for 10 bits ADC and $\|\mathbf{J}_1\| = 27$, $\|\mathbf{J}_2\| = 19$, $\|\mathbf{J}_3\| = 18$, $\|\mathbf{J}_4\| = 32$ test points for 12 bits ADC. The identification efficiency of newly found models is shown in Table 11.

It should be emphasized that after applying the described procedure (i.e., the proposed algorithm usage for the modified, digitalized form of the training patterns) the mathematical regression models have been adjusted and specialized to high precise identifications with limited test measure resolution presence. The accuracy achieved for 12 bits conversion is practically the same as the one presented previously in Table 9, i.e., determined without quantization noise consideration. It proved resistance of the described technique to practical degradation of A/D converted test signature. Additionally, the same test problem was checked for larger quant obtained after 10 bits very low-cost test response sampling and the performance parameters identification achievements are very promising again. The first section of identification reliability results from Table 11 shows that 10 bits A/D conversion process is enough, and it assured the identification accuracy much better than for the alternative previous method [24].

Table 10
The identification accuracy obtained after signatures quantization

	12 bit ADC			14 bit ADC		
	Avg. level [%]	Max. level [%]	Std. dev. [%]	Avg. level [%]	Max. level [%]	Std. dev. [%]
$\lvert K_{MX}\rvert$	3.007	12.799	2.020	0.937	3.103	0.680
$\lvert K_{400Hz}\rvert$	0.279	0.670	0.178	0.091	0.280	0.058
$\lvert K_{1300Hz}\rvert$	0.050	0.149	0.035	0.029	0.108	0.023
f_{BW}	0.669	1.633	0.391	0.297	1.107	0.212
Averagely:	**1.001**	**3.813**	**0.656**	**0.338**	**1.149**	**0.243**

Table 11
The proposed method accuracy for quantized signatures and corrected models

	10 bit ADC			12 bit ADC		
	Avg. level [%]	Max. level [%]	Std. dev. [%]	Avg. level [%]	Max. level [%]	Std. dev. [%]
$\lvert K_{MX}\rvert$	0.496	2.020	0.373	0.425	1.387	0.303
$\lvert K_{400Hz}\rvert$	0.147	0.424	0.111	0.048	0.236	0.041
$\lvert K_{1300Hz}\rvert$	0.084	0.264	0.066	0.051	0.205	0.036
f_{BW}	0.296	1.157	0.252	0.285	0.890	0.204
Averagely:	**0.256**	**0.966**	**0.201**	**0.202**	**0.680**	**0.146**

5. Conclusions

This paper presents the method for functional parameters estimation of analog circuits. The selected parameters (DC and maximal gain, frequency and phase shift at -3 dB and -20 dB attenuation points) are indirectly estimated based on analysis of time domain circuit responses (examples 4.1 and 4.2). Also, it is possible to perform successful fault detection of selected components in the tested circuit (example 4.1). The analysis uses multiple regression and has proven to be effective yet simple to implement in purely digital circuitry (low memory and computational requirements, small silicone area overhead). The analysis can be implemented in common system-on-chip blocks (A/D converters, FLASH memory), thus main functionality can be implemented in software. The testing method belongs to the simulation before testing (SBT) class, therefore on-line testing time (circuit excitation, response collection, response analysis) is minimized and does not depend on test preparation time (computational effort). It means the method can be effectively implemented as independent built-in self-test (BIST) or support for built-in testing (BIT). Excitation for tested analog circuit has the form of rectangular pulses, thus can be also generated in a purely digital way. The detailed form of the excitation (pulses pattern) is constructed by means of genetic optimization technique. Specific chromosome coding is used to further reduce the memory requirements of on-line analysis. The main goal is the maximization of effectiveness of parameters estimation or fault detection. The results are promising and show improvement comparing to the previous work.

Acknowledgements. This paper is supported by the Polish Ministry of Science and Higher Education funding for statutory activities.

REFERENCES

[1] J.L. Huertas, "Test and design for testability of analog and mixed-signal IC: theoretical basic and pragmatical approaches", in *European Conference On Circuit Theory And Design*, Davos, Switzerland, 1993, pp. 75–156.

[2] L. Milorand and A.L. Sangiovanni-Vincentelli, "Minimizing production test time to detect faults in analog circuits", *IEEE Trans. Comput-Aided Des. Integr. Circuits Syst.* 13 (6), 796–813 (1994).

[3] K. Baker, A.M. Richardson, and A.P. Dorey, "Mixed signal test-techniques, applications and demands", in *IEE Proceedings - Circuits, Devices and Systems* 143 (6), 358–365, 1996, doi: 10.1049/ip-cds:19960904.

[4] A. Milne, D. Taylor, and K. Naylor, "Assessing and comparing fault coverage when testing analogue circuits", in *IEE Proceedings – Circuits, Devices and Systems* 144 (1), 1–4, 1997, doi: 10.1049/ip-cds:19970870.

[5] J. Savir and Z. Guo, "Test Limitations of Parametric Faults In Analog Circuits", *IEEE Trans. Instrum. Meas.* 52 (5), 1444–1454 (2003).

[6] M. Tadeusiewicz, S. Hałgas, and M. Korzybski, "Multiple catastrophic fault diagnosis of analog circuits considering the component tolerances", *Int. J. Circuit Theory Appl.* 40 (10), 1041–1052 (2012).

[7] D. Grzechca, T. Golonek, and J. Rutkowski, "Analog Fault AC Dictionary Creation – The Fuzzy Set Approach", in *IEEE International Symposium on Circ. and Syst.*, Kos, Greece, 2006, pp. 5744–5747.

[8] M. Tadeusiewicz and S. Hałgas, "A method for multiple soft fault diagnosis of linear analog circuits", *Measurement*, 131, 714–722 (2019).

[9] M. Tadeusiewicz and S. Hałgas, "Soft fault diagnosis of linear circuits with the special attention paid to the circuits containing current conveyors", *AEU-Int. J. Electron. Commun.* 115 (2019).

[10] H. Dai and M. Souders, "Time domain testing strategies and fault diagnosis for analog systems", in *IEEE Instrumentation and Measurement Technology Conference*, 1989, pp. 293–298.

[11] A. Balivada, J. Chen, and J.A. Abraham, "Analog testing with time response parameters", *IEEE Des. Test Comput.* 13(2), 18–25 (1996).

[12] Ł. Chruszczyk and J. Rutkowski, "Specialised excitation and wavelet feature extraction in fault diagnosis of analog electronic circuits", in *IEEE International Conference on Electronics, Circuits and Systems*, Malta, 2008, pp. 242–246.

[13] S. Temich, T. Golonek, and D. Grzechca, "Design an Identification Function to Reduce the Computational Resources on the Testing Process of an Analog Electronic Circuit", *Elektron. Elektrotech.* 25 (3), 25–33 (2019).

[14] D. Grzechca and Ł. Chruszczyk, "Wavelet – Neural Network to Analog Paramteric Fault Circuit Location", *13-th International Mixed Signals Testing Workshop and 3rd GHz/Gbps Test Workshop*, Povoa de Varzim, Portugal, 2–6 (2007).

[15] S. Hałgas, "Multiple soft fault diagnosis of nonlinear circuits using the fault dictionary approach", *Bull. Pol. Ac.: Tech.* 56 (1), 53–57 (2008).

[16] P. Jantos, D. Grzechca, and J. Rutkowski, "Evolutionary algorithms for global parametric fault diagnosis in analogue integrated circuits", *Bull. Pol. Ac.: Tech.* 60 (1), 133–142 (2012).

[17] M. Woźniak and D. Połap, "On Some Aspects of Genetic and Evolutionary Methods for Optimization Purposes", *Int. J. Electron. and Telecomm. (IJET)*, 61 (1), 7–16 (2015).

[18] M. Tadeusiewicz and S. Hałgas, "A fault verification method for testing of analogue electronic circuits", *Metrol. Meas. Syst.*, 25 (2), 331–346 (2018).

[19] M. Tadeusiewicz and S. Hałgas, "A method for fault diagnosis of nonlinear circuits", *Compel-Int. J. Comp. Math. Electr. Electron. Eng.* 38 (6), 1770–1781 (2019).

[20] D.E. Goldberg, *Genetic Algorithms in Search, Optimization & Machine Learning*, Addison-Wesley, 1989.

[21] Z. Michalewicz, *Genetic Algorithms + Data Structures = Evolution Programs*, Springer-Verlag, 1996.

[22] D. MacKay, *Information Theory, Inference and Learning Algorithms*, CUP, 2003.

[23] T. Golonek and J. Rutkowski, "Genetic-algorithm-based method for optimal analog test points selection", *IEEE Trans. Circuits Syst. II-Express Briefs* 54 (2), 117–121 (2007).

[24] T. Golonek and J. Machniewski, "Analog Circuit Specification Testing by Means of Walsh–Hadamard Transform and Multiple Regression Supported by Evolutionary Computations", *Circuits Syst. Signal Process.* 37 (7), 2736–2771 (2018).

[25] P.N. Variyam, S. Cherubal, and A. Chatterjee, "Prediction of analog performance parameters using fast transient testing", *IEEE Trans. Comput-Aided Des. Integr. Circuits Syst.* 21(3), 349–361 (2002).

[26] P.N. Variyam and A. Chatterjee, "Specification-driven test generation for analog circuits", *IEEE Trans. Comput-Aided Des. Integr. Circuits Syst.* 19 (10), 1189–1201 (2000). doi: 10.1109/43.875320.

[27] D. De Venuto, E. Cantatore, G. Gramegna, C. Marzocca, and F. Corsi, "An Approach to the Specification Driven Testing of Analogue Circuits", IEEE Mediterranean Electrotechnical Conference on Industrial Applications in Power Systems, Computer Science and Telecommunications, Italy, 1283–1286 (1996).

[28] A. Sen and M. Srivastava, Regression Analysis – Theory, Methods, and Applications, Springer-Verlag, Berlin, 2011.

[29] B. Kamińska *et al.*, "Analog and mixed-signal benchmark circuits – first release", in *IEEE International Test Conference*, Washington, USA, 1997, pp. 183–190.

[30] R. Kondagunturi, E. Bradley, K. Maggard, and C. Stroud, "Benchmark circuits for analog and mixed-signal testing", in *IEEE Southeastcon 99 Conference on Technology on the Brink of 2000*, Lexington, 1999, pp. 217–220.

[31] B. Long, M. Li, H. Wang, and S. Tian, "Diagnostics of analog circuits based on LS-SVM using time domain features", *Circuits Syst. Signal Process.* 32 (6), 2683–2706 (2013).

[32] A.D. Spyronasios, M.G. Dimopoulos, and A.A. Hatzopoulos, "Wavelet Energy-based Mahalanobis Distance Metric for Testing Analog and Mixed-Signal Circuits", in *IEEE International Conference Mixed Design of Integrated Circuits and Systems*, Warsaw, 2010, pp. 218–224.

[33] S.R. Das *et al.*, "Testing analog and mixed-signal circuits with built-in hardware – A new approach", in *IEEE Trans. Instrum. Meas.* 56 (3), 840–855 (2007).

[34] T.R. Balen, J.V. Calvano, M.S. Lubaszewski, and M. Renovell, "Built-in self-test of field programmable analog arrays based on transient response analysis", *J. Electron. Test.-Theory Appl.* 23 (6), 497–512 (2007).

[35] M. Lubaszewski and J.L. Huertas, "Test and Design-for-Test of Mixed-Signal Integrated Circuits", in *Information Technology*, R. Reis (Ed.), vol. 157, IFIP International Federation for Information Processing, Springer, Boston, 2004, pp. 183–212.